

Lanthanide(III)/Actinide(III) Differentiation in Mixed Cyclopentadienyl/Dithiolene Compounds from X-ray Diffraction and Density Functional Theory Analysis

Mathieu Roger,[†] Lotfi Belkhiri,[‡] Pierre Thuéry,[†] Thérèse Arliguie,^{*,†}
Marc Fourmigué,[§] Abdou Boucekkine,^{*,||} and Michel Ephritikhine^{*,†}

Service de Chimie Moléculaire, DSM, DRECAM, CNRS URA 331, CEA Saclay, 91191 Gif-sur-Yvette, France, Laboratoire de Chimie des Matériaux (LCM), Département de Chimie, Faculté des Sciences, Université Mentouri de Constantine, BP 325, Route de l'aéroport Ain El Bey, Constantine 25017, Algérie, Laboratoire de Chimie, Ingénierie Moléculaire et Matériaux (CIMMA) UMR 6200, CNRS-Université d'Angers, 2 Bd. Lavoisier, 49045 Angers, France, and Laboratoire de Chimie du Solide et Inorganique Moléculaire (LCSIM), Institut de Chimie de Rennes, UMR 6511, CNRS-Université de Rennes 1, 35042 Rennes, France

Received April 26, 2005

Treatment of $[\text{U}(\text{Cp}^*)_2\text{Cl}_2]$ with Na_2dddt in thf afforded the “ate” complex $[\text{U}(\text{Cp}^*)_2\text{Cl}(\text{dddt})\text{Na}(\text{thf})_2]$ (**1**), and the salt-free compound $[\text{U}(\text{Cp}^*)_2(\text{dddt})]$ (**2**) could be extracted from **1** with toluene ($\text{Cp}^* = \eta\text{-C}_5\text{Me}_5$; dddt = 5,6-dihydro-1,4-dithiin-2,3-dithiolate). Reduction of **2** with $\text{Na}(\text{Hg})$ or addition of Na_2dddt to $[\text{U}(\text{Cp}^*)_2\text{Cl}_2\text{Na}(\text{thf})_x]$ in the presence of 18-crown-6 gave the first uranium(III) dithiolene compound, $[\text{Na}(18\text{-crown-6})(\text{thf})_2][\text{U}(\text{Cp}^*)_2(\text{dddt})]$ (**4**). The dimeric lanthanide complexes $\{[\text{Ln}(\text{Cp}^*)_2(\text{dddt})\text{K}(\text{thf})_2]_2\}$ ($\text{Ln} = \text{Ce}$ (**5**), Nd (**6**)) were prepared by reaction of $[\text{Ln}(\text{Cp}^*)_2\text{Cl}_2\text{K}]$ with K_2dddt , and in the presence of 15-crown-5, they were transformed into the cation–anion pairs $[\text{K}(15\text{-crown-5})_2][\text{Ln}(\text{Cp}^*)_2(\text{dddt})]$ ($\text{Ln} = \text{Ce}$ (**7**), Nd (**8**)). The crystal structures of **2**, **4**·thf, **5**–**7**, **7**·0.5(pentane), and **8**·0.5(pentane) were determined by X-ray diffraction analysis. Comparison of the structural parameters of the anions $[\text{M}(\text{Cp}^*)_2(\text{dddt})]^-$ ($\text{M} = \text{U}, \text{Ce}, \text{Nd}$) revealed that the U–S and U–C(Cp^*) distances are shorter than those expected from a purely ionic bonding model; the relatively small folding of the dddt ligand suggests that the interaction between the C=C double bond and the metal center is weak, in agreement with the NMR observations in solution. The structural data obtained from molecular geometry optimizations on the complexes $[\text{M}(\text{Cp}^*)_2(\text{dddt})]^{-,0}$ ($\text{M} = \text{Ce}, \text{U}$) using relativistic density functional theory (DFT) calculations reproduce experimental trends. A detailed orbital analysis shows that the contraction of the metal–sulfur bond lengths when passing from $[\text{Ce}(\text{Cp}^*)_2(\text{dddt})]^-$ to $[\text{U}(\text{Cp}^*)_2(\text{dddt})]^-$ is partly related to the uranium 5f orbital–ligand mixing, which is greater than the cerium 4f orbital–ligand mixing. The comparison of the two $[\text{U}(\text{Cp}^*)_2(\text{dddt})]^{-,0}$ species reveals a higher ligand-to-metal donation in the case of the U(IV) complex.

Introduction

Dithiolene complexes of the d transition metals have gained a prominent position in coordination chemistry, justified by the rich diversity of their structures, their unusual redox reactivity, their significant role in certain metalloenzyme reactions, and their remarkable conductivity and optical or magnetic properties in the solid state.¹ The introduction of the f elements in these types of complexes seemed interesting to us in view of their paramagnetism, structural flexibility, and redox behav-

ior, which could favor the emergence of novel structures and electronic interactions. We recently reported on a variety of tris(dithiolene) complexes of cerium and neodymium which adopt mononuclear, infinite chain, or honeycomb network crystal structures.² Our attempts to prepare analogous compounds of uranium(III) were unsuccessful, due to their inherent instability toward oxidation, but we isolated homoleptic tris- and tetrakis(dithiolene) complexes of uranium(IV).³ We have also been interested in organouranium compounds with dithiolene ligands and first characterized a number of neutral mono(cyclooctatetraenyl)uranium(IV) complexes of the general formula $\{[\text{U}(\text{COT})(\text{dithiolene})_2]_2\}$ or $[\text{U}(\text{COT})(\text{dithiolene})(\text{L})_2]$ ($\text{COT} = \eta\text{-C}_8\text{H}_8$; $\text{L} = \text{Lewis base}$)⁴ and the dianionic complex $[\text{Na}(18\text{-crown-6})(\text{thf})_2]_2^-$

* To whom correspondence should be addressed. E-mail: arliguie@drecam.cea.fr (T.A.); abdou.boucekkine@univ-rennes1.fr (A.B.); ephri@drecam.cea.fr (M.E.).

[†] CEA Saclay.

[‡] Université Mentouri de Constantine.

[§] CNRS-Université d'Angers.

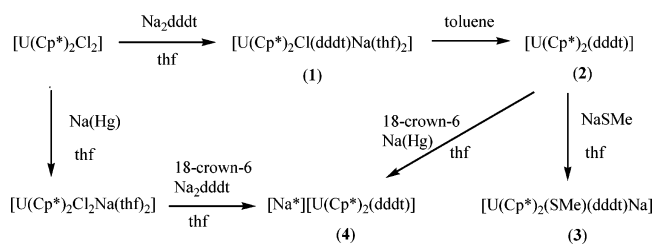
^{||} CNRS-Université de Rennes.

(1) (a) *Prog. Inorg. Chem.* **2004**, *52* (Dithiolene Chemistry: Synthesis, Properties and Applications; Stiefel, E. I., Ed.; special volume). (b) Cassoux, P.; Valade, L.; Kobayashi, H.; Kobayashi, A.; Clark, R. A.; Underhill, A. E. *Coord. Chem. Rev.* **1991**, *110*, 115. (c) Olk, R. M.; Olk, B.; Dietzsh, W.; Kirmse, R.; Hoyer, E. *Coord. Chem. Rev.* **1992**, *117*, 99.

(2) Roger, M.; Arliguie, T.; Thuéry, P.; Fourmigué, M.; Ephritikhine, M. *Inorg. Chem.* **2005**, *44*, 584.

(3) Roger, M.; Arliguie, T.; Thuéry, P.; Fourmigué, M.; Ephritikhine, M. *Inorg. Chem.* **2005**, *44*, 594.

(4) (a) Arliguie, T.; Thuéry, P.; Fourmigué, M.; Ephritikhine, M. *Organometallics* **2003**, *22*, 3000. (b) Arliguie, T.; Thuéry, P.; Fourmigué, M.; Ephritikhine, M. *Eur. J. Inorg. Chem.* **2004**, 4502.

Scheme 1. Synthesis of the Uranium Complexes^a

^a Na* = Na(18-crown-6)(thf)₂.

[U(COT)(dddt)₂] (dddt = 5,6-dihydro-1,4-dithiin-2,3-dithiolate), precursor of the corresponding monoanionic derivative [Na(18-crown-6)(thf)][U(COT)(dddt)₂], a unique example of an uranium(V) complex with metal–sulfur bonds.⁵ However, we were unable to isolate any compound of uranium(III) in this class of mono(cyclooctatetraenyl) derivatives. We then turned our attention to the family of bis(pentamethylcyclopentadienyl) complexes, which are regarded as models in organo-f-element chemistry.⁶ In this paper we report in detail the synthesis and characterization of [U(Cp*)₂(dddt)] (Cp* = η-C₅Me₅)⁵ and its derivatives, including [Na(18-crown-6)(thf)₂][U(Cp*)₂(dddt)], the first dithiolene complex of uranium(III); we also present the first organolanthanide complexes with a dithiolene ligand, [{Ln(Cp*)₂(dddt)K(thf)₂]₂] and [K(15-crown-5)]₂[Ln(Cp*)₂(dddt)] (Ln = Ce, Nd), which are compared with their uranium(III) counterpart. The significant differences in the molecular structures of the analogous U(IV), U(III), and Ln(III) compounds, deduced from single-crystal X-ray diffraction analysis, are discussed in light of theoretical calculations using the Kohn–Sham formalism of DFT in its relativistic formulation. A molecular orbital analysis could bring to light the major metal–ligand orbital interactions leading to lanthanide/actinide differentiation. In particular, the important role of f orbitals will be investigated.

Results and Discussion

Synthesis of the Complexes. The most classical synthesis of mixed cyclopentadienyl/dithiolene compounds of d transition metals consists of treating halide precursors with the dithiolene salt.⁷ Such displacement reactions are often complicated in f-element chemistry by the tedious elimination of salts and pervasive formation of anionic addition complexes in place of simple metathesis products. Indeed, treatment of [U(Cp*)₂Cl₂]⁸ with 1 equiv of Na₂dddt in thf readily gave the “ate” complex [U(Cp*)₂Cl(dddt)Na(thf)₂] (**1**), isolated as a brown powder in 76% yield (Scheme 1). The salt-free compound [U(Cp*)₂(dddt)] (**2**) could be extracted from **1** with toluene, and brown crystals of **2** suitable for X-ray diffraction analysis were deposited from a benzene solution. In contrast, **2** could not be obtained from [U(Cp*)₂Cl(dddt)K(thf)_x], which remains stable in a toluene suspension. The capacity of **2** to retain alkali-

metal salts in its coordination sphere was also illustrated by the addition of NaSMe, to give a brown powder of [U(Cp*)₂(SMe)(dddt)Na] (**3**) in 58% yield.

Addition of M₂dddt to the uranium(III) dichloride [U(Cp*)₂Cl₂M(thf)_x] (M = Na, K)⁹ gave a mixture of complexes containing a major component, presumably [U(Cp*)₂(dddt)M(thf)_x]; no pure compound was isolated from this mixture. The same reactions in the presence of 18-crown-6 led to the clean formation of the anionic complex [U(Cp*)₂(dddt)]⁻; dark brown crystals of [Na(18-crown-6)(thf)₂][U(Cp*)₂(dddt)]·thf (**4**·thf) were obtained in 67% yield upon slow diffusion of pentane into a thf solution, and their structure was determined by X-ray crystallography. Complex **4** was alternatively synthesized by Na(Hg) reduction of **2** in the presence of 18-crown-6 and was transformed back into **2** by oxidation with AgBPh₄; **2** was inert toward the silver salt. A number of neutral bis(cyclopentadienyl) dithiolene complexes of the group 4 and 5 metals were found by cyclic voltammetry to undergo reversible one-electron reduction,⁷ but **4** is, to the best of our knowledge, the first example of such a low-valent compound with a negative charge and the metal center in the formal +3 oxidation state to have been isolated. However, **4** was not very stable at room temperature, both in solution and in the solid state, and decomposed into unidentified products with release of pentamethylcyclopentadiene.

The “ate” complexes [Ln(Cp*)₂Cl₂K(thf)_n] are classical precursors to bis(pentamethylcyclopentadienyl)lanthanide compounds. However, we did not succeed in preparing the cerium and neodymium derivatives [Ce(Cp*)₂Cl₂K(thf)_n] (n = 1, 2)^{10,11,12} and [Nd(Cp*)₂Cl₂K(thf)₂]¹² by following the published procedures. In order to reach completion, reactions of CeCl₃ or NdCl₃ with 2 equiv of KCp* in thf required much higher temperature and/or longer times as compared to those reported in the literature; this difference is perhaps not surprising for a heterogeneous reaction and is likely due to distinct physical forms of solid LnCl₃ and KCp* in thf suspension. The solvent-free compounds [Ln(Cp*)₂Cl₂K] (Ln = Ce, Nd) were isolated as a purple and blue powders, in 40 and 70% yields, respectively. The purple cerium complex is easily distinguishable from the previously reported yellow derivative [Ce(Cp*)₂Cl₂K(thf)],¹² which was indeed obtained at the first stage of the drying process.

Treatment of [Ln(Cp*)₂Cl₂K] with 1 equiv of K₂dddt in thf afforded the dithiolene complexes [{Ln(Cp*)₂(dddt)K(thf)₂]₂] (Ln = Ce (**5**), Nd (**6**)) (Scheme 2). The reaction mixture was stirred for 12 h (Ln = Ce) or 5 days (Ln = Nd) at 20 °C, and the red powder of **5** and green powder of **6** were recovered in 76 and 51% yields, respectively. Recrystallization from thf gave single crystals, and the dimeric structure of these compounds is described below.

(9) Fagan, P. J.; Manriquez, J. M.; Marks, T. J.; Day, C. S.; Vollmer, S. H.; Day, V. W. *Organometallics* **1982**, *1*, 170.

(10) Evans, W. J.; Olofson, J. M.; Zhang, H.; Atwood, J. L. *Organometallics* **1988**, *7*, 629.

(11) (a) Raush, M. D.; Moriarity, K. J.; Atwood, J. L.; Weeks, J. A.; Hunter, W. E.; Brittain, H. G. *Organometallics* **1986**, *5*, 1281. (b) Hazin, P. N.; Huffman, J. C.; Bruno, J. W. *Organometallics* **1987**, *6*, 23. (c) Renkema, J.; Teuben, J. H. *Recl. Trav. Chim. Pays-Bas* **1986**, *105*, 241.

(12) Evans, W. J.; Keyer, R. A.; Ziller, J. W. *Organometallics* **1993**, *12*, 2618.

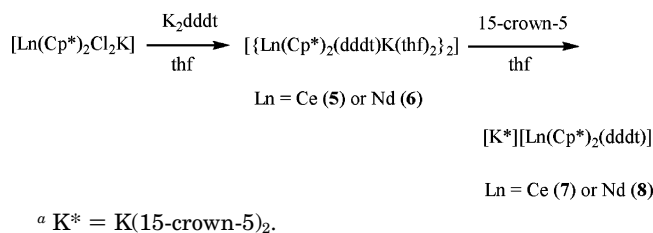
(5) Arliguie, T.; Fourmigué, M.; Ephritikhine, M. *Organometallics* **2000**, *19*, 109.

(6) Edelmann, F. In *Comprehensive Organometallic Chemistry*; Abel, E. W., Stone, F. G. A., Wilkinson, G., Eds.; Pergamon: Oxford, U.K., 1995; Vol. 4, Chapter 2, p 11.

(7) Fourmigué, M. *Coord. Chem. Rev.* **1998**, *180*, 823.

(8) Fagan, P. J.; Manriquez, J. M.; Maatta, E. A.; Seyam, A. M.; Marks, T. J. *J. Am. Chem. Soc.* **1981**, *103*, 6650.

Scheme 2. Synthesis of the Lanthanide Complexes^a



For meaningful structural comparison with the uranium(III) complex **4**, crystals of $[\text{M}(18\text{-crown-6})(\text{thf})_2][\text{Ln}(\text{Cp}^*)_2(\text{dddt})]$ (M = Na, K) were desirable. No crystals suitable for X-ray diffraction analysis were obtained upon slow diffusion of pentane into a thf solution of **5** or **6** and 18-crown-6. K/Na exchange in $[\text{Ln}(\text{Cp}^*)_2\text{Cl}_2\text{K}]$ with excess NaBr, followed by reaction with Na₂dddt in thf, led to the sodium analogues of **5** and **6**, $[\text{Ln}(\text{Cp}^*)_2(\text{dddt})\text{Na}(\text{thf})_x]$, and addition of 18-crown-6 afforded crystals of the expected complexes which, in contrast to **4**, are quite stable at room temperature. Unfortunately, the structural parameters were measured with low accuracy because of extended disorder in the crown ether and thf ligands. Eventually, replacement of 18-crown-6 with 15-crown-5 induced the crystallization of $[\text{K}(15\text{-crown-5})_2][\text{Ln}(\text{Cp}^*)_2(\text{dddt})]$ (Ln = Ce (**7**), Nd (**8**)); the structures of the pink crystals of **7** and **7**·0.5(pentane) and green crystals of **8**·0.5(pentane) are described below. Attempts to grow single crystals of the uranium analogue of **7** and **8** incorporating the same $[\text{K}(15\text{-crown-5})_2]^+$ cation were unsuccessful.

Satisfactory elemental analyses (C, H, S) were obtained for all the complexes, except **8**. Compounds **1**–**8** were characterized by their ¹H NMR spectra. In contrast to what is observed with the analogous group 4 d⁰ compounds,^{7,13} the spectra showed that, even at –80 °C, the two Cp* rings were equivalent, as well as the protons of the methylene groups of the dddt ligand, indicating that the ring inversion process related to the folding of the metallacycle along the S–S axis is much easier in these f-element complexes.

Crystal Structures of the Complexes. The structures of $[\text{U}(\text{Cp}^*)_2(\text{dddt})]$ and $[\text{M}(\text{Cp}^*)_2(\text{dddt})]^-$ (M = U, Ce, Nd) will be presented and discussed together, after those of the dimeric compounds $[\{\text{Ln}(\text{Cp}^*)_2(\text{dddt})\text{K}(\text{thf})_2\}_2]$ (Ln = Ce (**5**), Nd (**6**)). The latter are isomorphous, and a view of the cerium derivative is shown in Figure 1; selected bond distances and angles are listed in Table 1. The centrosymmetric dimer is built up from two $\text{Ln}(\text{Cp}^*)_2(\text{dddt})$ units which are bridged by two $\text{K}(\text{thf})_2$ fragments. The lanthanide atom is in the pseudo-tetrahedral environment which is quite invariably found in the $[\text{M}(\text{Cp}^*)_2\text{X}_2]$ type complexes, in particular the bis(cyclopentadienyl) dithiolene compounds of the d transition metals.⁷ In agreement with the variation in the ionic radii of the trivalent Ce and Nd ions,¹⁴ the Ce–S and Ce–C(Cp*) distances are longer, by ca. 0.03 Å, than the Nd–S and Nd–C(Cp*) distances. The Ce–S and Nd–S bond lengths, with average values of 2.838(13) and 2.806(10) Å, respec-

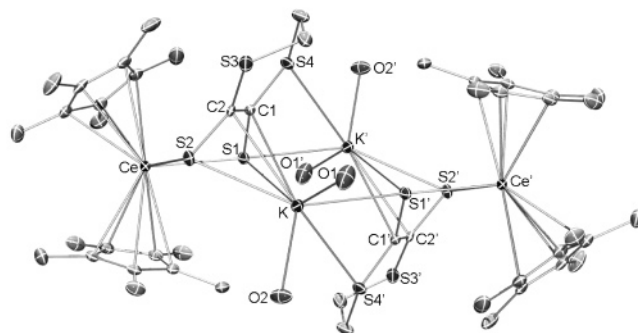


Figure 1. View of $[\{\text{Ce}(\text{Cp}^*)_2(\text{dddt})\text{K}(\text{thf})_2\}_2]$ (**5**). The carbon atoms of the tetrahydrofuran molecules and the hydrogen atoms have been omitted for clarity. Displacement ellipsoids are drawn at the 40% probability level. Primed atoms are related to unprimed ones by the symmetry center.

tively, are smaller than those measured in the tris(dithiolene) complexes of cerium and neodymium, 2.92(2) Å in $\{[\text{Na}_2(18\text{-crown-6})\text{Na}(\text{py})_2\text{Ce}(\text{dddt})_3(\text{py})\cdot 3\text{py}]\}_\infty$ and 2.90(3) Å in $\{[\text{K}_3(18\text{-crown-6})_{1.5}\text{Nd}(\text{dddt})_3(\text{py})\cdot 3\text{py}]\}_\infty$,² in line with this shortening of the Ln–S bond, the chelate bite angles S(1)–Ln–S(2), 73.96(2) and 74.49(2)° in **5** and **6** respectively, are larger by ca. 4°. The S₄C₂ fragment of the dddt ligand is planar with an rms deviation of ca. 0.075 Å; the folding angles θ , defined as the dihedral angle between the S(1)–Ln–S(2) plane and the mean S(1)–C(1)–C(2)–S(2) plane, are equal to 53.65(7) and 52.22(5)° in **5** and **6**, respectively. These folding angles are much smaller than those of 65–82° found in the aforementioned tris(dithiolene) complexes, reflecting a weaker interaction between the C=C double bond of the dithiolene ligand and the metal center. The Ln–C(1) and Ln–C(2) distances, which vary from 3.370(3) to 3.424(3) Å, are indeed larger than those measured in the series of tris(dithiolene) complexes of cerium and neodymium, which range between 2.881(7) and 3.3388(5) Å with an average value of 3.1(2) Å.² The bridging $\text{K}(\text{thf})_2$ fragment is bound to the S(1), S(2), C(1), and C(2) atoms of one dddt ligand and to the S(1) and S(4) atoms of the other one. The average K–S distances of 3.26(5) and 3.27(5) Å in **5** and **6**, respectively, are similar to those of 3.22(5) Å in $\{[\text{K}_3(18\text{-crown-6})_{1.5}\text{Nd}(\text{dddt})_3(\text{py})\cdot 3\text{py}]\}_\infty$ ² and 3.2558(1) Å in $[\text{K}(18\text{-crown-6})\text{-(NC}_5\text{H}_4\text{S-2)}]$.¹⁵ The K–C distances in **5** and **6** vary from 3.020(3) to 3.156(3) Å, with an average value of 3.09(6) Å, which can be compared with those found in the gallium N-heterocyclic carbene analogues $[\{(\text{L})\text{KGa}(\text{RN}=\text{CH})_2\}_2]$ (2.999(4) Å for L = tmeda and R = Bu^t, 3.012(5) Å for L = tmeda and R = C₆H₃(Prⁱ)₂, 2.99(1) Å for L = Et₂O and R = C₆H₃(Prⁱ)₂)¹⁶ or the 1,4-cyclohexa-2,5-dienyl lanthanide compounds $[\text{K}(18\text{-crown-6})(\mu\text{-}\eta^2\text{:}\eta^2\text{-C}_6\text{H}_6)\text{Ln}\{\text{C}_5\text{H}_3(\text{SiMe}_3)_2\}_2]$ (3.2(1) Å for Ln = La,¹⁷ Ce,¹⁷ Nd¹⁸); these distances are shorter than the typical value of 3.4–3.5 Å measured in a number of compounds which exhibit a cation– π interaction between a potassium cation and an aromatic moiety.¹⁹

(15) Chadwick, S.; Ruhlandt-Senge, K. *Chem. Eur. J.* **1998**, *4*, 1768.

(16) Baker, R. J.; Farley, R. D.; Jones, C.; Kloth, M.; Murphy, D. M. *Dalton Trans.* **2002**, 3844.

(17) Cassani, M. C.; Gun'ko, Y. K.; Hitchcock, P. B.; Lappert, M. F. *Chem. Commun.* **1996**, 1987.

(18) Cassani, M. C.; Gun'ko, Y. K.; Hitchcock, P. B.; Lappert, M. F.; Laschi, F. *Organometallics* **1999**, *18*, 5539.

(13) (a) Guyon, F.; Lenoir, C.; Fourmigué, M.; Larsen, J.; Amaudrut, J. *Bull. Soc. Chim. Fr.* **1994**, *131*, 217. (b) Domercq, B.; Coulon, C.; Fourmigué, M. *Inorg. Chem.* **2001**, *40*, 371.

(14) Shannon, R. D. *Acta Crystallogr., Sect. A* **1976**, *32*, 751.

Table 1. Selected Bond Lengths (Å) and Angles (deg) in $[\{\text{Ln}(\text{Cp}^*)_2(\text{ddd})\}\text{K}(\text{thf})_2]_2$ (Ln = Ce, Nd)

	Ln = Ce	Ln = Nd		Ln = Ce	Ln = Nd
Ln–S(1)	2.8253(8)	2.7958(9)	S(1)–C(1)	1.774(3)	1.769(3)
Ln–S(2)	2.8510(8)	2.8168(9)	S(2)–C(2)	1.771(3)	1.766(3)
$\langle \text{Ln}–\text{C}(\text{Cp}^*) \rangle^a$	2.807(13)	2.766(13)	S(3)–C(2)	1.772(3)	1.774(3)
Ln–C(1)	3.370(3)	3.370(3)	S(4)–C(1)	1.778(3)	1.773(3)
Ln–C(2)	3.424(3)	3.411(3)	C(1)–C(2)	1.351(4)	1.355(4)
K–S(1)	3.3212(11)	3.3408(12)	K–C(1)	3.156(3)	3.142(3)
K–S(2)	3.2012(10)	3.2080(11)	K–C(2)	3.038(3)	3.020(3)
K–S(1')	3.2415(10)	3.2578(10)	K–O(1)	2.672(3)	2.671(3)
K–S(4')	3.2958(10)	3.2894(11)	K–O(2)	2.655(2)	2.653(2)
$\text{Cp}^*–\text{Ln}–\text{Cp}^*$	134.1	133.7	S(1')–K–S(4')	51.82(5)	51.75(2)
S(1)–Ln–S(2)	73.96(2)	74.49(2)	O(1)–K–O(2)	82.63(8)	82.61(9)
S(1)–K–S(2)	63.10(2)	62.45(2)	θ^a	53.65(7)	52.22(5)

^a Cp^* is the centroid of the cyclopentadienyl ligand, and θ is the folding angle of the ddd ligand. Primed atoms are related to unprimed ones by the symmetry center.

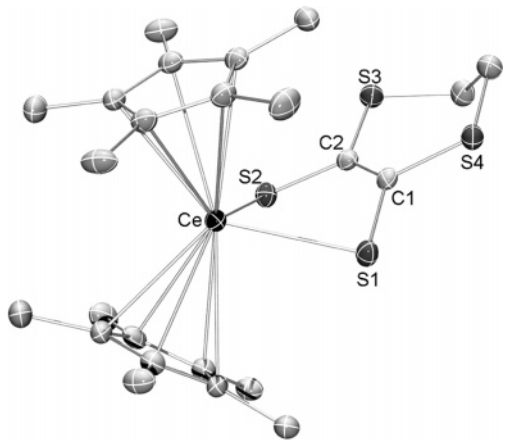


Figure 2. View of the anion $[\text{Ce}(\text{Cp}^*)_2(\text{ddd})]^-$ in **7**. The hydrogen atoms have been omitted for clarity. Displacement ellipsoids are drawn at the 30% probability level.

The molecular structures of the neutral compound $[\text{U}(\text{Cp}^*)_2(\text{ddd})]$ (**2**) and of the anions $[\text{U}(\text{Cp}^*)_2(\text{ddd})]^-$ in **4**·thf, $[\text{Ce}(\text{Cp}^*)_2(\text{ddd})]^-$ in **7** or **7**·0.5(pentane), and $[\text{Nd}(\text{Cp}^*)_2(\text{ddd})]^-$ in **8**·0.5(pentane) are similar and resemble those of the bis(cyclopentadienyl) dithiolene complexes of the d transition metals.⁷ A view of the cerium anion in **7** is shown in Figure 2, and selected bond distances and angles are listed in Table 2. A major objective of this work was to compare the structural parameters of analogous U(III) and Ln(III) dithiolene complexes, within the scope of studies devoted to the differentiation of trivalent lanthanide and actinide complexes.^{20,21} The differences in bond distances and angles in such compounds are expected to be small, and because the uranium derivative is not isomorphous with its cerium and neodymium congeners, it is imperative to be sure that modifications in the crystal structures of these complexes are not caused by distinct intermo-

lecular contacts or packing forces. Weak intermolecular C–H···S interactions are present in the structures of **2**, **4**, **7**, and **8**, with H···S distances typically equal to 2.9 Å. In contrast, S···S contacts are observed only for one of the two independent $[\text{Ln}(\text{Cp}^*)_2(\text{ddd})]^-$ anions in the isomorphous complexes **7**·0.5(pentane) and **8**·0.5(pentane), where S(3B) is separated from S(3B') in a symmetry-related anion by 3.911 and 3.812 Å, for Ln = Ce(2), Nd(2), respectively; these short contacts are similar to those found between the cations $[\text{W}(\text{C}_5\text{H}_5)_2(\text{ddd})]^{+}$ (3.730 Å) and $[\text{W}(\text{C}_5\text{H}_4\text{Bu}^t)_2(\text{C}_3\text{S}_5)]^{+}$ (3.793 and 3.811 Å).²² These intermolecular S···S interactions have an influence on the folding angle θ and the Ln(2)–C(1) and Ln(2)–C(2) distances, which are respectively larger, by ca. 8°, and shorter, by ca. 0.15 Å, than those found in the other $[\text{Ln}(\text{Cp}^*)_2(\text{ddd})]^-$ anions, with Ln = Ce(1), Nd(1) in **7**·0.5(pentane) or **8**·0.5(pentane) and Ln = Ce in **7**. The crystal structures of the latter, which seem not to be perturbed by external constraints, could thus be compared with that of the uranium complex **4**.

The U–S bond lengths in **2**, which average 2.640(11) and 2.633(3) Å for the two independent and quite identical molecules present in the asymmetric unit, are in the range of those determined for terminally coordinated thiolate ligands in uranium(IV) complexes, which vary from 2.58(1) Å in $[\text{U}_3(\text{S})(\text{S}^t\text{Bu})_{10}]^{23}$ to 2.759(3) Å in $[\text{Net}_2\text{H}_2]_2[\text{U}(\text{SPh})_6]$.²⁴ These distances are shorter than those found in the other uranium(IV) dithiolene compounds: 2.720(3)–2.859(3) Å in the series of mono(cyclooctatetraenyl) complexes $[\text{U}(\text{COT})(\text{dithiolene})(\text{L})_2]^{4}$ and 2.737(14) Å in the homoleptic complex $[\text{Na}(18\text{-crown-6})(\text{py})_2]_2[\text{U}(\text{ddd})_3]$.³ As expected from the difference between the radii of the U(III) and U(IV) ions, $r(\text{U}^{\text{III}})$ and $r(\text{U}^{\text{IV}})$,¹⁴ the U–S bond lengths in the anion $[\text{U}(\text{Cp}^*)_2(\text{ddd})]^-$ of **4** as well as the U–C(Cp^*) distances, which average 2.79(2) Å, are larger than the corresponding distances in **2**, by ca. 0.13 and 0.06 Å, respectively. Also in agreement with the distinct ionic radii $r(\text{Ln}^{\text{III}})$ of Ce(III) and Nd(III), the average Ce–S and Ce–C(Cp^*) distances, respectively equal to 2.794(19) and 2.822(6) Å for both **7** and **7**·0.5(pentane), are ca. 0.04 Å longer than the average Nd–S and Nd–C(Cp^*) distances in **8**·0.5(pentane) (2.753(8) and 2.778(6) Å, respectively). The Ln–S distances in the $[\text{Ln}(\text{Cp}^*)_2(\text{ddd})]^-$ anions are 0.04 Å larger than those

(19) (a) Hitchcock, P. B.; Lappert, M. F.; Lawless, G. A.; Royo, B. *J. Chem. Soc., Chem. Commun.* **1993**, 554. (b) Ugozzoli, F.; Ori, O.; Casnati, A.; Pochini, A.; Ungaro, R.; Reinhoudt, D. N. *Supramol. Chem.* **1995**, *5*, 179. (c) Cassani, M. C.; Duncalf, D. J.; Lappert, M. F. *J. Am. Chem. Soc.* **1998**, *120*, 12958. (d) Gun'ko, Y.; Hitchcock, P. B.; Lappert, M. F. *Chem. Commun.* **1998**, 1843.

(20) (a) Berthet, J. C.; Nierlich, M.; Ephritikhine, M. *Polyhedron* **2003**, *22*, 3475. (b) Cendrowski-Guillaume, S. M.; Le Gland, G.; Nierlich, M.; Ephritikhine, M. *Eur. J. Inorg. Chem.* **2003**, 1388. (c) Karmazin, L.; Mazzanti, M.; Bezombes, J. P.; Gateau, C.; Pécaut, J. *Inorg. Chem.* **2004**, *43*, 5147. (d) Mehdoui, T.; Berthet, J. C.; Thuéry, P.; Ephritikhine, M. *Dalton Trans.* **2004**, 579. (e) Mehdoui, T.; Berthet, J. C.; Thuéry, P.; Ephritikhine, M. *Eur. J. Inorg. Chem.* **2004**, 1996. (f) Villiers, C.; Thuéry, P.; Ephritikhine, M. *Eur. J. Inorg. Chem.* **2004**, 4624.

(21) Berthet, J. C.; Miquel, Y.; Iveson, P. B.; Nierlich, M.; Thuéry, P.; Madic, C.; Ephritikhine, M. *Dalton Trans.* **2002**, 3265.

(22) Jourdain, I. V.; Fourmigué, M.; Guyon, F.; Amaudrut, J. *J. Chem. Soc., Dalton Trans.* **1998**, 483.

(23) Leverd, P. C.; Arliguie, T.; Ephritikhine, M.; Nierlich, M.; Lance, M.; Vigner, J. *New J. Chem.* **1993**, *17*, 769.

(24) Leverd, P. C.; Lance, M.; Nierlich, M.; Vigner, J.; Ephritikhine, M. *J. Chem. Soc., Dalton Trans.* **1994**, 3563.

Table 2. Selected Bond Lengths (Å) and Angles (deg) in [U(Cp*)₂(dddt)] and the Anions [M(Cp*)₂(dddt)]⁻ (M = U, Ce, Nd)

	[U(Cp*) ₂ (dddt)] (2) ^a	[U(Cp*) ₂ (dddt)] ⁻ in 4 ·thf	[Ce(Cp*) ₂ (dddt)] ⁻ in 7	[Ce(Cp*) ₂ (dddt)] ⁻ in 7 ·0.5(pentane) ^b	[Nd(Cp*) ₂ (dddt)] ⁻ in 8 ·0.5(pentane) ^b
M–S(1)	2.629(3) [2.633(3)]	2.7807(16)	2.8081(14)	2.7984(16), 2.7753(19)	2.7661(17), 2.7477(19)
M–S(2)	2.650(3)	2.7661(17)	2.8255(15)	2.7703(17), 2.7848(18)	2.7449(18), 2.754(2)
⟨M–C(Cp*) ^c ⟩	2.73(2) [2.732(17)]	2.79(2)	2.82(2)	2.815(17), 2.83(2)	2.772(18), 2.784(17)
M–C(1)	3.147(11) [3.142(9)]	3.360(6)	3.423(5)	3.392(6), 3.251(7)	3.385(6), 3.284(7)
M–C(2)	3.165(11)	3.307(6)	3.449(5)	3.370(6), 3.235(7)	3.369(6), 3.253(7)
S(1)–C(1)	1.735(12) [1.756(11)]	1.763(7)	1.767(6)	1.767(7), 1.777(8)	1.768(7), 1.781(7)
S(2)–C(2)	1.769(14)	1.770(7)	1.770(6)	1.770(7), 1.759(7)	1.776(7), 1.768(7)
S(3)–C(2)	1.764(12)	1.791(7)	1.775(6)	1.792(7), 1.775(7)	1.778(7), 1.773(7)
S(4)–C(1)	1.756(13) [1.747(11)]	1.775(6)	1.785(6)	1.781(7), 1.774(7)	1.787(7), 1.768(7)
C(1)–C(2)	1.363(19) [1.36(3)]	1.355(9)	1.354(8)	1.344(10), 1.359(11)	1.349(10), 1.354(10)
Cp*–M–Cp* ^c	133.1 [134.4]	135.7	135.4	135.5, 134.7	134.6, 135.0
S(1)–M–S(2)	78.93(12) [79.37(16)]	76.24(5)	75.45(4)	76.19(5), 77.48(6)	76.65(5), 78.01(6)
θ ^c	56.23(25) [56.36(36)]	51.92(16)	46.76(12)	48.42(16), 56.86(19)	47.46(15), 53.61(20)

^a Values in brackets are the corresponding values in the second independent molecule, which possesses a plane of symmetry. ^b The two values given are for the two independent anions with the atoms of the dddt ligands labeled A and B, respectively. ^c Cp* is the centroid of the cyclopentadienyl ligand, and θ is the folding angle of the dddt ligand.

in the dimeric compounds **5** and **6**, in relation to the distinct coordination modes, terminal or bridging, of the dddt ligand.

Comparison of the structures of the [U(Cp*)₂(dddt)]⁻ and [Ln(Cp*)₂(dddt)]⁻ anions reveals that the average U–S and U–C(Cp*) distances in **4** are shorter than those expected from a purely ionic bonding model; their values, 2.773(7) and 2.79(2) Å, are ca. 0.02–0.03 Å smaller than the average Ce–S and Ce–C(Cp*) distances, while $r(\text{U}^{\text{III}})$ is 0.01 Å larger than $r(\text{Ce}^{\text{III}})$. This shortening of the U–S and U–C bond lengths with respect to the Ln–S and Ln–C distances most probably reflects a stronger interaction between the actinide and both the dithiolene and cyclopentadienyl ligands, in relation to the more covalent character of the bonding. The better affinity of neutral nitrogen and phosphorus ligands or anionic cyclopentadienyl and iodide groups for U(III) than for Ln(III) ions has been similarly assessed from the crystal structures of analogous complexes, by measuring the deviations Δ between the differences ⟨U–X⟩ – ⟨Ln–X⟩ and $r(\text{U}^{\text{III}}) - r(\text{Ln}^{\text{III}})$.^{20,21,25} These deviations are generally equal to 0.02–0.05 Å but are as high as 0.1 Å in the phosphorus complexes [M(C₅H₄Me)₃(L)] (M = Ce, U; L = PMe₃, P(OCH₂)₃CEt)²⁵ and in the tris(btp) compounds [M(btp)₃]₃ (M = La, Ce, Sm, U; btp = (2,6-dialkyl-1,2,4-triazin-3-yl)pyridine);²¹ this greatest deviation was explained by the softer character and better π-accepting ability of the phosphine, phosphite, and btp ligands. In view of the pronounced softness of the sulfur atom, the Δ value of 0.03 Å can be considered small; the same deviation was observed in the crown thioether complexes [MI₃(1,4,7-trithiacyclononane)(MeCN)₂] (M = U, La), the only other analogous 4f- and 5f-element compounds with a sulfur ligand to have been crystallographically characterized.²⁶

The structures of the [U(Cp*)₂(dddt)] molecule and the [M(Cp*)₂(dddt)]⁻ anions (M = U, Ce, Nd) show that the S₄C₂ planar part of the dddt ligand is folded along the S(1)–S(2) axis, with respect to the S(1)–M–S(2) plane. The average folding angles θ are 56.3(3) and 51.92(16)° in the uranium(IV) and -(III) complexes,

respectively, and 47.5(8)° in the lanthanide derivatives, excluding the higher values found in one of the two independent anions in **7**·0.5(pentane) and **8**·0.5(pentane) (56.86(19) and 53.61(20)°, respectively), which, as noted above, likely result from constraints due to intermolecular S···S interactions. As in the case of the dimeric complexes **5** and **6**, these angles are much smaller than those of 65–82° found in the tris(dithiolene) compounds of uranium(IV), cerium(III), and neodymium(III)^{2,3} and the series of mono(cyclooctatetraenyl) complexes [U(COT)(dithiolene)(L)₂].⁴ The relatively low values of the θ angles could be related to the weaker interaction between the C=C double bond of the dddt ligand and the metal center and the more facile dithiolene ring inversion, in agreement with the NMR observations in solution (vide supra). The ⟨U–C(1,2)⟩ average bond length of 3.151(9) Å in the two independent molecules of **2** is significantly shorter, by ca. 0.2 Å, than the value of 3.33(3) Å in the uranium(III) congener **4**. In keeping with previous studies on dithiolene complexes of the d-block transition metals, this difference would reflect the lower electron density on the U(IV) center, which strengthens the interaction with the dithiolene ligand.^{13,27} However, this ⟨U–C(1,2)⟩ distance is larger than those encountered in the homoleptic tris(dithiolene) compounds of U(IV), which are typically equal to 2.9 Å, confirming that the interaction between the metal and the C=C double bond of the dddt ligand is relatively weak.

In all the complexes, the characteristics of the dddt ligands, such as the C(sp²)–S distances, which vary from 1.735(12) to 1.792(7) Å, and the C=C distances, which lie between 1.344(10) and 1.363(19) Å, exhibit no significant variation and are consistent with those found in the other uranium and lanthanide dithiolene compounds. The structures of the cations [Na(18-crown-6)-(thf)₂] and [K(15-crown-5)₂] are unexceptional, being identical with those found, for example, in [Na(18-crown-6)(thf)₂][U(Cp*)₂(SiPr)₂]²⁸ and [K(15-crown-5)₂][C₅H₅].²⁹

(25) Brennan, J. G.; Stults, S. D.; Andersen, R. A.; Zalkin, A. *Organometallics* **1988**, *7*, 1329.

(26) Karmazin, L.; Mazzanti, M.; Pécaut, J. *Chem. Commun.* **2002**, 654.

(27) (a) Fourmigué, M. *Acc. Chem. Res.* **2004**, *37*, 179. (b) Lauher, J. W.; Hoffman, R. J. *Am. Chem. Soc.* **1976**, *98*, 1729.

(28) Arliguie, T.; Lescop, C.; Ventelon, L.; Leverd, P. C.; Thuéry, P.; Nierlich, M.; Ephritikhine, M. *Organometallics* **2001**, *20*, 3698.

(29) Cole, M. L.; Jones, C.; Junk, P. C. *Dalton Trans.* **2002**, 896.

Table 3. Mean Experimental and Calculated Bond Lengths (Å) and Angles (deg) in the $[M(\text{Cp}^*)_2(\text{dddt})]^{-1,0}$ ($M = \text{Ce}, \text{U}$) Complexes

structure	spin state		M–Cp* ^a	C–C(Cp)	M–S	S–C	M–(C ₁ =C ₂) ^b	C=C	Cp*–M–Cp*	S–M–S	θ ^c	TBE (eV)
[Ce(Cp* ₂ (dddt))] [–] (Ce(III))	doublet	calcd	2.602–2.625	1.426–1.431	2.848	1.777	3.306	1.369	132.5	75.6	51.9	–361.038 ^D
		exptl	2.539–2.563		2.794	1.769	3.340	1.352	135.2	76.3	47.5	
[U(Cp* ₂ (dddt))] [–] (U(III))	quartet	calcd	2.474–2.532	1.428–1.434	2.764	1.774	3.166	1.373	132.0	78.1	54.3	–362.744 ^Q
		exptl	2.506–2.529		2.773	1.767	3.264	1.355	135.7	76.2	51.9	
[U(Cp* ₂ (dddt))] (U(IV))	triplet	calcd	2.490–2.503	1.426–1.435	2.674	1.774	3.115	1.376	131.5	78.8	55.1	–361.415 ^T
		exptl	2.455–2.458		2.636	1.754	3.111	1.361	133.7	79.6	56.3	

^a Distances between the metal and the two Cp* centroids. ^b Distance between the metal and the middle of the dddt C=C double bond. ^c Metallacycle folding angle.

Density Functional Theory Calculations. Several $[M(\text{Cp}^*)_2\text{dddt}]^{-1,0}$ complexes ($M = \text{Ce}, \text{U}$) complexes were calculated. The structures of the complexes were fully optimized without any symmetry constraint. The initial conformations of the complexes were deduced from the crystallographic data. Some of the complexes exhibit open-shell structures with metallic $4f^n$ and $5f^n$ ground-state configurations for cerium and uranium, respectively. In the case of the latter compounds, several different low-lying spin states can be considered according to the different possible electronic 5f orbital occupations. For all complexes, we considered the highest spin state as the ground state, this state being correctly described by a single Kohn–Sham determinantal wave function. In addition, for the 5f orbitals there are typically degeneracies or near-degeneracies present in a molecule, which make it difficult to achieve convergence in the self-consistent solution of the Kohn–Sham equations.^{30a} For this reason we have chosen to start our study by spin-restricted calculations; in this case, the electronic density is computed by considering the possibly unpaired electrons to be equally split between the α and β molecular spin-orbitals. Moreover, to assist SCF convergence, the “smearing” recipe allowing the 5f electrons to spread over a wide range of 5f orbitals, thus leading to nonintegral MO occupancies, has been applied. This recipe has been already successfully applied to organoactinide compounds.^{30b} This approach has a questionable physical significance, but without electron smearing, the SCF procedure oscillates wildly and convergence can hardly be achieved. At the converged geometry, the highest MOs which are very close energetically to one another were obtained, respecting an Aufbau electronic structure. These MOs are found to be almost entirely of a metallic 4f and 5f character for cerium and uranium complexes, respectively. Then, starting with the restricted geometry, we carried out a second geometry optimization within a spin-unrestricted calculation, considering the highest spin state for each compound. We found that the geometries computed at the spin-unrestricted level are very close to the re-

stricted ones. Energetically the highest spin state is always more stable than the fictitious spin-restricted one.

Molecular Geometry Optimizations. The geometries of the $[M(\text{Cp}^*)_2(\text{dddt})]^{-}$ anionic species ($M = \text{Ce}, \text{U}$) and of the neutral $[U(\text{Cp}^*)_2(\text{dddt})]$ complex were fully optimized without any constraint of symmetry. Table 3 reports the spin-unrestricted computed metal–ligand distances and bond angles, compared to the experimental values available from the crystal structures. In the last column of this table is given the total bonding energy (TBE), which is defined as the difference between the energy of the molecule and that of its constituting atoms, the latter being in an averaged (spherically symmetric and spin-restricted) ground state.³¹ We note that the energy difference between the two uranium complexes in Table 3 is small (equal to 1.33 eV), indicating the facile electrochemical interconversion between these two species.

The spin-unrestricted optimized geometries are in good agreement with the experimental structures. Comparison of the computed $[M(\text{Cp}^*)_2(\text{dddt})]^{-}$ anionic complexes of cerium and uranium, the metals being in the +3 oxidation state, shows that these two complexes have very similar molecular geometries (Figure 3). The observed U–ligand/Ce–ligand bond length contraction³² is also well reproduced by the DFT calculations, which show, as found experimentally, that the M–Cp* and M–S distances are significantly longer for $M = \text{Ce}$ than for $M = \text{U}$. This result is not obvious, since the ionic radius of U(III) is 0.01 Å, larger than that of Ce(III).¹⁴ In contrast, comparing the anionic $[U(\text{Cp}^*)_2(\text{dddt})]^{-}$ and neutral $[U(\text{Cp}^*)_2(\text{dddt})]$ complexes, the U–S and U–(C₁=C₂) distances are found to be shorter for U(IV) than for U(III), following the ionic radii of the metal ions. Moreover, the slight increase of the C=C bond length (1.355 to 1.361 Å) from U(III) to U(IV) is to be noted (Table 3). The calculated angle values are also in good agreement with the experimental data. This confirms the reliability of the ZORA-BP86/TZP approach in the prediction of the molecular geometries and conformations of organoactinide compounds.³³

(30) (a) Schreckenbach, G.; Hay, J. P.; Martin, R. L. *J. Comput. Chem.* **1999**, *20*, 7090. (b) Cloke, F. G. N.; Green, J. C.; Kaltsoyannis, N. *Organometallics* **2004**, *23*, 832. (c) Li, J.; Bursten, B. E. *J. Am. Chem. Soc.* **1998**, *120*, 11456. (d) Li, J.; Bursten, B. E. *J. Am. Chem. Soc.* **1999**, *121*, 10243. (e) Cloke, F. G. N.; Green, J. C.; Jardine, C. N. *Organometallics* **1999**, *18*, 1080. (f) Lu, H.; Li, L. *Theor. Chem. Acc.* **1999**, *102*, 121. (g) Ricciardi, G.; Rosa, A.; Baerends, E. J.; van Gisbergen, S. A. J. *J. Am. Chem. Soc.* **2002**, *124*, 12319. (h) O’Grady, E.; Kaltsoyannis, N. *J. Chem. Soc., Dalton Trans.* **2002**, 1233. (i) Castro-Rodriguez, I.; Olsen, K.; Gantzel, P.; Meyer, K. *J. Am. Chem. Soc.* **2003**, *125*, 4565. (j) Kaltsoyannis, N. *Chem. Soc. Rev.* **2003**, *32*, 9. (k) Guillaumont, D. *J. Phys. Chem. A* **2004**, *108*, 6893.

(31) (a) te Velde, G.; Bickelhaupt, F. M.; van Gisbergen, S. A. J.; Fonseca Guerra, C.; Baerends, E. J.; Snijders, J. G.; Ziegler, T. *J. Comput. Chem.* **2001**, *931*. (b) Fonseca Guerra, C.; Snijders, J. G.; te Velde, G.; Baerends, E. J. *Theor. Chem. Acc.* **1998**, 391. (c) ADF2004.01; SCM, Theoretical Chemistry, Vrije Universiteit, Amsterdam, The Netherlands; <http://www.scm.com>.

(32) (a) Pyykkö, P. *Chem. Rev.* **1988**, *88*, 563. (b) Kaltsoyannis, N. *J. Chem. Soc., Dalton Trans.* **1997**, 1.

(33) (a) van Lenthe, E.; Baerends, E. J.; Snijders, J. G. *J. Chem. Phys.* **1993**, *99*, 4597. (b) van Lenthe, E.; Baerends, E. J.; Snijders, J. G. *J. Chem. Phys.* **1994**, *101*, 9783. (c) van Lenthe, E.; Ehlers, A.; Baerends, E. J. *J. Chem. Phys.* **1999**, *110*, 8943.

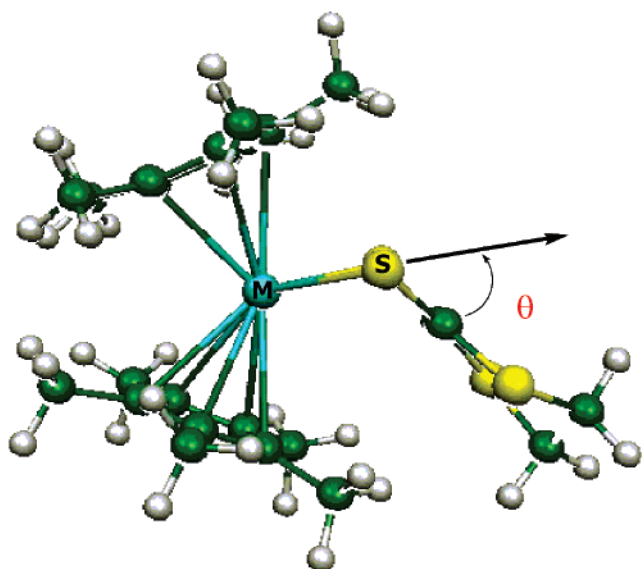


Figure 3. Optimized molecular geometry of $[\text{U}(\text{Cp}^*)_2(\text{ddd})]^-$.

Perhaps the most striking feature of the complexes under consideration is that their crystal structures exhibit a folded MS_2C_2 metallacycle, as shown in Figure 3. This structural feature is related to the facile dithiolene ring inversion revealed by NMR observations in solution. Furthermore, it is worth noting that the experimental folding angles θ average $50\text{--}55^\circ$ for the uranium and cerium dddt complexes, whereas those observed for analogous d^0 Cp^*_2ddd transition-metal complexes are much lower ($20^\circ \leq \theta \leq 30^\circ$).^{7,13} Moreover, this folding angle θ varies with the uranium ion charge, $56.3(3)$ and $51.92(16)^\circ$, as measured respectively for the U(IV) and U(III) complexes. It is satisfying to find that the computed (gas phase) US_2C_2 folding angle satisfactorily fits the experimental (crystal) value. Indeed, the increase of this angle from 47.5° up to 51.9 and 56.3° on going from the cerium species to the uranium ones is correctly reproduced by the computed values, namely 51.9 , 54.3 , and 55.1° . In a parallel direction, the $\text{M}-(\text{C}_1=\text{C}_2)$ distance decreases in this series, as can be seen in Table 3. However, these folding angles remain rather small compared to those observed in the homoleptic dithiolene complexes of uranium(IV)³ and in the series of mono(cyclooctatetraenyl)uranium dithiolene complexes.^{4,5} Therefore, we have performed DFT calculations to study the energy profile of this folding process in the case of the $[\text{U}(\text{Cp}^*)_2(\text{ddd})]^-$ complex. We found that a variation of this angle by $\pm 10^\circ$ in the gas phase around the energy minimum requires less than 1 kcal mol^{-1} . The metallacycle flexibility permits the $\text{C}=\text{C}$ bond of the dddt ligand to come close to the U(III) center without a loss in the $\text{U}-\text{S}$ bond strength. However, this flexibility is limited by the overcrowding Cp^* ligands around the central atom. Indeed, after carrying out a geometry optimization of the $[\text{U}(\text{Cp})_2(\text{ddd})]^-$ complex, taking non-methylated cyclopentadienyl groups, we found a much larger θ value, equal to 75.1° , and a very short $\text{M}-(\text{C}_1=\text{C}_2)$ distance, equal to 2.811 \AA , allowing a metallacycle conformation similar to that observed in the aforementioned homoleptic and mono(cyclooctatetraenyl) compounds.

Molecular Orbital Analysis. The covalent bonding

in these systems can be described in terms of a ligand-to-metal donation, involving the filled ligand σ and π molecular orbitals and the empty metal ns , $(n-1)d$, and $(n-2)f$ orbitals (with $n=7$ for U and $n=6$ for Ce) and metal-to-ligand back-donation from the partially filled metal $4f$ or $5f$ orbitals to the empty ligand π^* molecular orbitals.

According to this, we present in Figure 4 a simplified (restricted) MO interaction diagram in which the numbered frontier MO energy levels are reported for the two anionic complexes $[\text{Cp}^*_2\text{M}(\text{ddd})]^-$ ($\text{M} = \text{Ce}, \text{U}$), as obtained via our unrestricted calculations. In this diagram, we represent also the main frontier MOs of the two interacting fragments Cp^*_2M^+ and ddd^{2-} , which are considered and give the metal atomic orbital contributions to each MO. The percentages $s/d/f/\text{Cp}_2\text{M}/\text{ddd}$ represent respectively the s , d , and f metal orbital contributions to the MOs, as well as the global contributions of the Cp^*_2M^+ and ddd^{2-} fragments. The energy gaps between different MO blocks are also indicated in this figure. We note that the number of valence electrons is not the same in the two complexes, because we considered different (Ce.5p) and (U.5d) frozen cores.

In $[\text{Ce}(\text{Cp}^*)_2(\text{ddd})]^-$, almost all the highest occupied MOs have a metal contribution less than or equal to 5%, indicating a very small cerium–ligand covalent bonding character with a more important contribution of $5d$ orbitals relative to $4f$ ones. The SOMO, which is a pure $4f$ orbital, remains localized on the cerium metal. This situation parallels that observed in $[\text{Ti}(\text{Cp}^*)_2(\text{ddd})]^-$ complexes. In contrast, for the uranium anion complex, ligand-to-metal donation is found to be more marked in a wide range of MOs. The highest in energy are pure $5f$ orbitals bearing three electrons localized on the uranium metal. The #83 bonding MO and those which are lower in energy involve mainly the σ and π ligand orbitals but also the empty metal $6d$ and $5f$ orbitals, with practically no participation from the uranium $7s$ orbitals. It is worth noting that the uranium contributions to the occupied MOs are more important than those of cerium. The total contribution of U(III) to the bonding MOs is several percent greater than the participation of Ce(III). The contraction of the metal–sulfur bond lengths on going from the cerium to the uranium anionic complex is partly related to the uranium $5f$ orbital–ligand mixing which is greater than the cerium $4f$ orbital–ligand mixing. This question will be discussed later in the text. To summarize, covalency is more present in the uranium complex through a slightly more marked ligand-to-metal electron donation between dithiolene ddd^{2-} and the metallic fragment Cp^*_2M^+ as well as back-donation from the metal to this ligand.

A more detailed MO interaction diagram for the $[\text{U}(\text{Cp}^*)_2(\text{ddd})]^-$ complex is exhibited in Figure 5. The complex is built up from its two fragments Cp^*_2U^+ and ddd^{2-} . As seen before in Figure 4, the Cp^*_2U^+ fragment bears low-lying MOs, namely partially occupied f -block levels, which can interact with the empty ones in the dithiolene ligand. When the ddd^{2-} ligand takes its usual coordination mode ($\theta = 50\text{--}55^\circ$), it is bound to U(III) mostly through an interaction with a $5f$ orbital, as illustrated by MO #83. Distortion could weaken this interaction, but only slightly, because the main lobe of the $5f$ orbital exhibits a large spatial extension toward the incoming ligand so that, even at low θ value, the

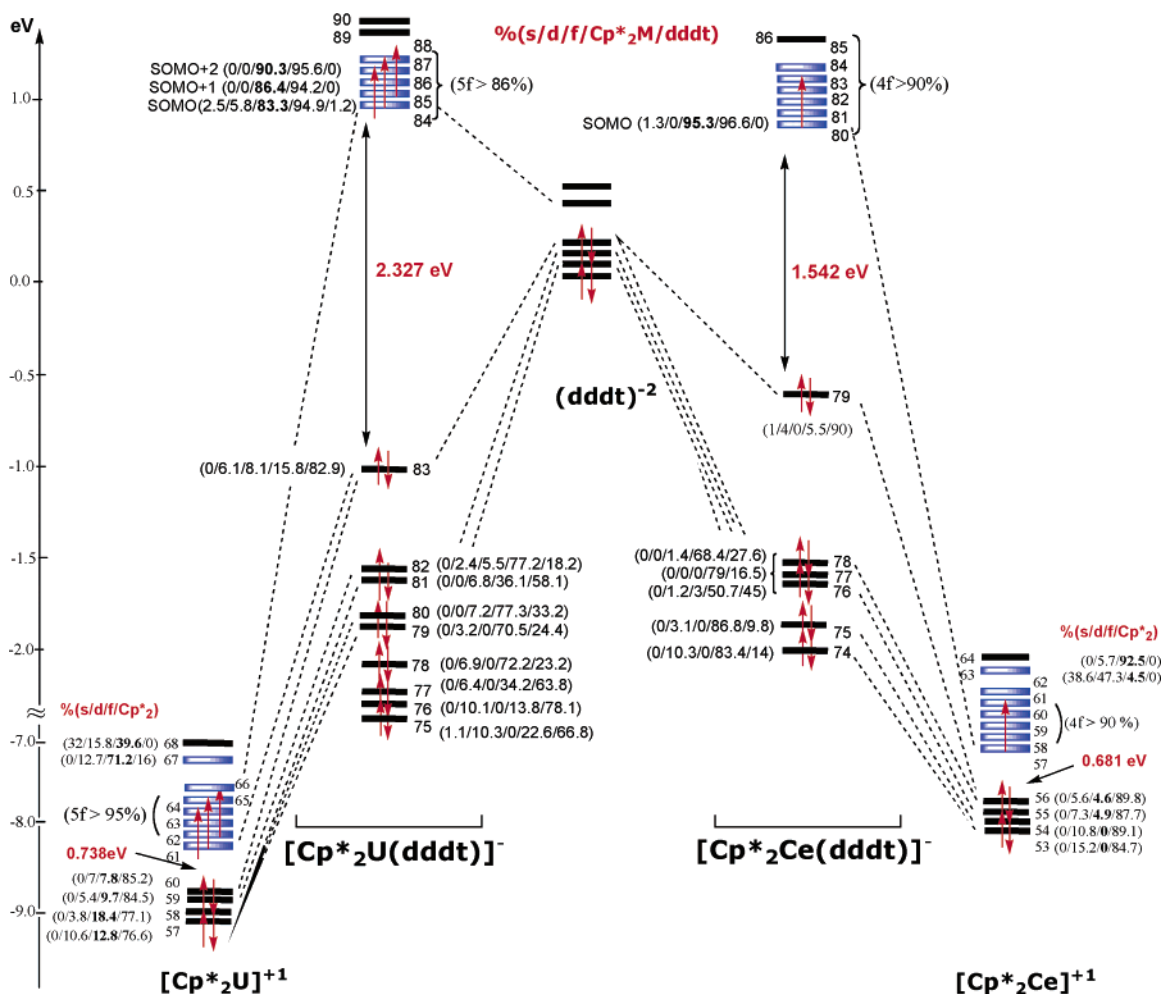


Figure 4. Frontier MO interaction diagram for the two $[M(\text{Cp}^*)_2(\text{ddd})]^-$ ($M = \text{Ce}, \text{U}$) complexes.

ddd^{2-} donor orbital can overlap well with it. This is the most striking aspect of the Cp^*_2U^+ fragment orbitals, which allow the U atom to develop a strong bonding interaction with the highly distorted dithiolene ligand. The presence of an analogous low-lying vacant nd orbital, in $d^{0,1}$ $[M(\text{Cp}^*)_2(\text{ddd})]$ complexes ($M = \text{Ti}, \text{Mo}, \text{W}$) may cause a similar ddd distortion, but the deformation, if any, would not be as large as in the actinide case, due to the smaller size of nd orbitals. This argument should provide a theoretical basis for understanding important aspects of the chemistry involving actinides compared to lanthanides and transition metals.

Electronic and Molecular Structure Comparison of $[M(\text{Cp}^*)_2(\text{ddd})]^{-0}$ ($M = \text{Ce}, \text{U}$) Complexes. Crystallographic studies have shown that the U–ligand bond lengths in $[\text{U}(\text{Cp}^*)_2(\text{ddd})]^-$ are shorter than the corresponding Ln–ligand bond distances in $[\text{Ln}(\text{Cp}^*)_2(\text{ddd})]^-$ ($\text{Ln} = \text{Ce}, \text{Nd}$). Furthermore, the deviation of the U– Cp^* and U–S bond lengths from a purely ionic bonding model is consistent with the presence of a stronger covalent interaction between the actinide and both the dithiolene and cyclopentadienyl ligands.

To understand these structural features and to get a further insight into the electronic structures of the $[M(\text{Cp}^*)_2(\text{ddd})]^{-0}$ ($M = \text{Ce}$ and U) complexes, we consider now their Mulliken population analysis. Although not very accurate, this population analysis may

indicate roughly the major charge transfers and bonding interactions occurring in a molecule. The results, gross orbital populations and atomic or ligand net charges, namely the net charge of the metal and sulfur (one) atoms and the total net charge of the Cp^*_2 group, are given in Table 4. The formal oxidation state of the metal ion as well as the number of unpaired electrons, i.e., the number of α electrons minus the number of β electrons (given by N) of each species are given in the second and third columns of the table. The metallic orbital populations within the α and β MOs and their sums are shown in the last four columns. It must be recalled that the Mulliken population analysis can produce nonphysical values as small negative orbital populations, and this is the case for the cerium orbitals. The metallic spin density (third column) is equal to the difference between the total atomic α and β populations of the metal. The results of our preliminary spin-restricted calculations, indicated by *RESTR*, are also given in this table. As it can be seen, the spin-restricted populations are very close to the unrestricted ones.

For all species, the Mulliken analysis clearly shows a diminution of the atomic net charge in comparison with the formal oxidation states +3 and +4, indicating the expected ligand-to-metal electron transfer. A rather low uranium net charge (+0.69) compared to that of cerium (+1.33) in the anionic complexes denotes an increased ligand-to-metal donation. Indeed, we see for

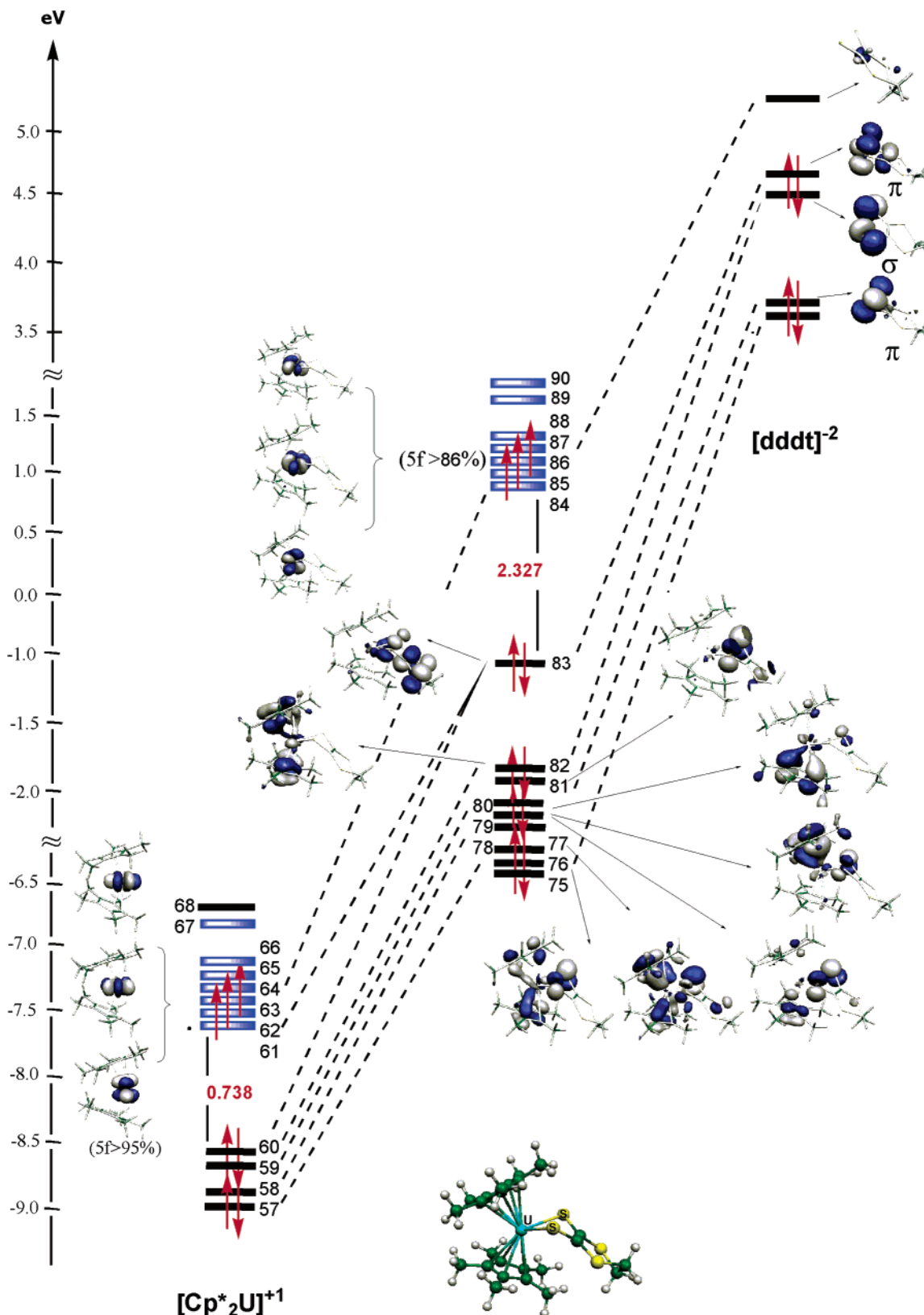


Figure 5. Frontier MOs of $[\text{U}(\text{Cp}^*)_2(\text{dddt})]^-$ and its two fragments under consideration.

instance that the Cp^*_2 ligands transfer more electrons to uranium than to cerium, since the net charge borne by these groups changes from -1.16 to -0.81 in the two complexes. However, the Mulliken analysis is known to be dependent on the atomic basis sets, and the large difference between U and Ce charges may be partly due

to basis set differences between U and Ce. Nevertheless, the difference between the net charges remains significant.

In the uranium complexes, the metallic charge decreases on passing from the anionic U(III) complex to the neutral U(IV) species, while the net charges of the

Table 4. Mulliken Population Analysis for [Ce(Cp*)₂(dddt)]⁻ and [U(Cp*)₂(dddt)]⁻⁰

structure	metal free ion	spin calcs	metal spin dens	metal net charge	ligand net charge			metal orbital pop.				
					S ⁻	Cp* ₂ ²⁻	spin	s* ^a	p* ^a	d	f	
[Ce ^{III} (Cp*) ₂ (dddt)] ⁻	Ce ³⁺ (4f ¹)							α	0.18	-0.11	0.66	1.12
								β	0.17	-0.10	0.61	0.14
		UNRESTR (N = 1) <i>RESTR</i>	1.01	+1.33 <i>+1.30</i>	-0.36 <i>-0.37</i>	-1.16 <i>-1.18</i>	α + β <i>0.37</i>	0.35 <i>-0.22</i>	-0.21 <i>1.27</i>	1.27 <i>1.26</i>	1.26 <i>1.26</i>	
[U ^{III} (Cp*) ₂ (dddt)] ⁻	U ³⁺ (5f ³)							α	1.18	3.09	0.92	2.95
								β	1.15	3.06	0.68	0.28
		UNRESTR (N = 3) <i>RESTR</i>	2.98	+0.69 <i>+0.57</i>	-0.21 <i>-0.17</i>	-0.81 <i>-0.56</i>	α + β <i>2.43</i>	2.33 <i>6.15</i>	6.15 <i>1.60</i>	1.60 <i>3.23</i>	3.23 <i>3.05</i>	
[U ^{IV} (Cp*) ₂ (dddt)]	U ⁴⁺ (5f ²)							α	1.18	3.10	0.97	2.57
								β	1.16	3.09	0.84	0.44
		UNRESTR (N = 2) <i>RESTR</i>	2.29	+0.65 <i>+0.60</i>	-0.10 <i>-0.09</i>	-0.15 <i>-0.11</i>	α + β <i>2.37</i>	2.34 <i>6.20</i>	6.19 <i>1.81</i>	1.81 <i>3.01</i>	3.01 <i>2.99</i>	

^a The atomic populations s* and p* refer to 6s/6p for cerium and 6s + 7s/6p + 7p for uranium.

Table 5. Calculated Mulliken Atom–Atom Overlap Populations

structure	spin	atom–atom overlap pop.					
		M–S	M–C(Cp)	M–Cp	C–C(Cp)	S–C	C=C
[Ce ^{III} (Cp*) ₂ (dddt)] ⁻	α	0.070–0.073	0.009–0.024	0.086	0.211–0.224	0.139–0.143	0.226
	β	0.049–0.055	0.008–0.020	0.073	0.217–0.227	0.140–0.144	0.228
	α + β	0.119–0.128	0.017–0.044	0.159	0.428–0.451	0.279–0.287	0.454
	<i>RESTR</i>	<i>0.112–0.134</i>	<i>0.016–0.039</i>	<i>0.143</i>	<i>0.432–0.458</i>	<i>0.260–0.270</i>	<i>0.453</i>
[U ^{III} (Cp*) ₂ (dddt)] ⁻	α	0.078–0.079	0.021–0.038	0.137	0.172–0.194	0.127–0.134	0.220
	β	0.063–0.067	0.003–0.026	0.060	0.204–0.216	0.139–0.141	0.219
	α + β	0.141–0.146	0.024–0.064	0.197	0.376–0.410	0.266–0.275	0.439
	<i>RESTR</i>	<i>0.146–0.152</i>	<i>0.018–0.058</i>	<i>0.173</i>	<i>0.355–0.417</i>	<i>0.273–0.280</i>	<i>0.390</i>
[U ^{IV} (Cp*) ₂ (dddt)]	α	0.076–0.086	0.018–0.037	0.126	0.174–0.199	0.133–0.139	0.196
	β	0.074–0.082	0.006–0.031	0.093	0.191–0.204	0.134–0.137	0.202
	α + β	0.150–0.168	0.024–0.068	0.219	0.365–0.403	0.267–0.276	0.398
	<i>RESTR</i>	<i>0.159–0.175</i>	<i>0.019–0.068</i>	<i>0.199</i>	<i>0.349–0.403</i>	<i>0.263–0.273</i>	<i>0.400</i>

sulfur atom and the Cp*₂ group increase, thus indicating that the higher uranium ionic charge in the neutral complex is compensated by a more important electronic donation from the ligands.

The metal spin densities are roughly equal to 1 and 3 for the Ce(III) and U(III) complexes, respectively. Moreover, the populations of the metallic f orbitals of these two species are slightly higher than 1 and 3. These values agree fairly well with the free metal ion configurations, which are 4f¹ for the former and 5f³ for the latter. The unrestricted calculations give a metallic spin density equal to 2.29 for the neutral uranium(IV) complex. Such a value obtained for a molecule in its triplet state, for which the number of unpaired electrons is 2, indicates that a small negative spin density is localized on the ligands. For this complex, it is noteworthy that the population of the uranium f orbitals is equal to 3.01, which is higher than that of the free U(IV) ion (5f²), as a consequence of the important ligand-to-metal donation. Comparison of the MOs of the two uranium complexes reveals that the contribution to the bonding of the 5f orbitals is more important for U(IV) than for U(III).

As expected, the overlap populations for the M–Cp* and M–S(dithiolene) bonds shown in Table 5 are rather large and bring to light the importance of covalent interactions in the complexes. This reflects also the good ability of Cp* and dddt ligands to coordinate 4f and 5f ions. In agreement with the computed charge transfers (Table 4) and the analysis of the MO interaction diagrams (Figure 4), the M–Cp* and M–S populations are found to be higher for M = U than for M = Ce.

Donation and Back-Donation. It is expected that the differentiation of lanthanide and actinide complexes for the same metal ion charge should come mainly from the larger size of the actinide ion and the greater extension of its 5f orbitals, which work as valence orbitals relative to the 4f lanthanide orbitals. In our case, we have seen more particularly how the latter parameter led to an enhanced interaction with the dddt ligand.

The calculated gross overlap populations between the metal ion and the five carbon atoms of the Cp* ring bring to light the stronger U–Cp* interactions relative to Ce–Cp*. This indicates a higher donating Cp* → U(III) effect, which results in a greater metallic charge stabilization. Moreover, the higher back-donating M → ligand capability of uranium which can populate the π* antibonding orbitals of the ligands appears when comparing the structural parameters of the cerium and uranium anionic complexes (Table 3), which show that the computed average C–C(Cp*) and C=C(dithiolene) bond lengths increase slightly from cerium to uranium. This is also well corroborated by the small decrease of the overlap population of the corresponding bonds reported in Table 5.

A direct interaction between the metallic ion and the C=C double bond of the dddt ligand could be considered to explain why the metallacycle is folded in these dithiolene complexes. However, the computed M–(C=C) overlap populations values remain very small or slightly negative. Indeed, a direct interaction between the dithiolene C=C double bond and the metal ion

seems unlikely, mainly because of the steric constraints due to the Cp* ligands, as seen before.

Conclusion

The synthesis of $[\text{K}(15\text{-crown-5})_2][\text{Ln}(\text{Cp}^*)_2(\text{dddt})]$ (Ln = Ce, Nd) and $[\text{Na}(18\text{-crown-6})(\text{thf})_2][\text{U}(\text{Cp}^*)_2(\text{dddt})]$, which are unique examples of organolanthanide complexes with a dithiolene ligand and of a dithiolene complex of uranium(III), permitted us to compare for the first time the structural parameters of analogous lanthanide(III) and actinide(III) compounds with anionic sulfur ligands. The shortening of the U–S bonds with respect to the Ln–S bonds is indicative of a stronger metal–sulfur interaction in the U(III) complex, due to the presence of a covalent contribution to the U–S bonding. Relativistic DFT calculations led to optimized geometries in good agreement with the crystallographic data for both the uranium and cerium complexes. While the complexes exhibit a folded MS_2C_2 metallacycle, the theoretical results indicate that a direct interaction between the dithiolene C=C double bond and the metal ion seems unlikely, mainly because of the steric constraints due to the Cp* ligands. Consideration of the orbital interactions between ligands and metals brings to light the importance of 5f uranium orbital mixing relative to the cerium 4f orbital mixing. Covalence contribution to the metal–sulfur bonds, as also described by overlap populations, is more important in uranium than in cerium complexes. Comparing the two uranium $[\text{U}(\text{Cp}^*)_2(\text{dddt})]^{-,0}$ complexes, it is also worth noting that ligand-to-metal donation is enhanced when passing from the U(III) to the U(IV) species.

Experimental Section

All reactions were carried out under argon (<5 ppm oxygen or water) using standard Schlenk-vessel and vacuum-line techniques or in a glovebox. Solvents were dried by standard methods and distilled immediately before use. The ^1H NMR spectra were recorded on a Bruker DPX 200 instrument and referenced internally using the residual protio solvent resonances relative to tetramethylsilane (δ 0). Elemental analyses were performed by Analytische Laboratorien at Lindlar (Germany). $[\text{U}(\text{Cp}^*)_2\text{Cl}_2]$,⁸ $[\text{U}(\text{Cp}^*)_2\text{Cl}_2\text{Na}(\text{thf})_2]$,⁹ K_2dddt , and Na_2dddt ¹³ were prepared according to literature procedures; CeCl_3 and NdCl_3 (Aldrich) were ground and dried under vacuum before use.

Synthesis of $[\text{U}(\text{Cp}^*)_2\text{Cl}(\text{dddt})\text{Na}(\text{thf})_2]$ (1). A flask was charged with $[\text{U}(\text{Cp}^*)_2\text{Cl}_2]$ (457 mg, 0.789 mmol) and Na_2dddt (178.5 mg, 0.789 mmol), and thf (50 mL) was condensed in. The reaction mixture was stirred at 20 °C for 2 h. After filtration, the solvent was evaporated off, leaving a brown residue which was washed with pentane (2 × 20 mL); the brown powder of **1** was dried under vacuum. Yield: 538 mg (76.5%). Anal. Calcd for $\text{C}_{32}\text{H}_{50}\text{ClNaO}_2\text{S}_4\text{U}$: C, 43.11; H, 5.65; S, 14.39. Found: C, 42.87; H, 5.53; S, 14.48. ^1H NMR (thf- d_8 , 23 °C): δ -1.32 (m, 2H, dddt), -1.40 (m, 2H, dddt), 11.02 (s, 30H, Cp*).

Synthesis of $[\text{U}(\text{Cp}^*)_2(\text{dddt})]$ (2). A flask was charged with $[\text{U}(\text{Cp}^*)_2\text{Cl}_2]$ (549 mg, 0.948 mmol) and Na_2dddt (214.6 mg, 0.948 mmol), and thf (50 mL) was condensed in. The reaction mixture was stirred at 20 °C for 2 h. After filtration, the solvent was evaporated off, leaving a brown residue of **1**, from which **2** was extracted with toluene (2 × 20 mL); the solvent was evaporated off and the product dried under vacuum. Yield: 458 mg (70%). Anal. Calcd for $\text{C}_{24}\text{H}_{34}\text{S}_4\text{U}$: C, 41.85; H, 4.98; S, 18.62. Found: C, 41.60; H,

4.82; S, 18.36. ^1H NMR (toluene- d_8 , 23 °C): δ -10.45 (s, 4H, dddt), 8.02 (s, 30H, Cp*). Crystals of **2** were obtained by crystallization from benzene.

Synthesis of $[\text{U}(\text{Cp}^*)_2(\text{SMe})(\text{dddt})\text{Na}]$ (3). A flask was charged with **2** (201.3 mg, 0.292 mmol) and NaSMe (41.0 mg, 0.585 mmol), and thf was condensed in. The reaction mixture was stirred at 20 °C for 2 h. After filtration, the solvent was evaporated off, leaving a brown residue, which was washed with pentane (2 × 20 mL); the brown powder of **3** was dried under vacuum. Yield: 128 mg (58%). Anal. Calcd. for $\text{C}_{25}\text{H}_{37}\text{NaS}_5\text{U}$: C, 39.57; H, 4.91; S, 21.13. Found: C, 39.42; H, 5.05; S, 20.88. ^1H NMR (thf- d_8 , 23 °C): δ -2.74 (s, 3H, SMe), 1.20 (m, 2H, dddt), 2.52 (m, 2H, dddt), 6.95 (s, 30H, Cp*).

Synthesis of $[\text{Na}(18\text{-crown-6})(\text{thf})_2][\text{U}(\text{Cp}^*)_2(\text{dddt})]$ (4). **Method 1.** A flask was charged with $[\text{U}(\text{Cp}^*)_2\text{Cl}_2]$ (80 mg, 0.138 mmol) and 2% Na(Hg) (334 mg, 0.291 mmol), and thf (20 mL) was condensed in. The reaction mixture was stirred at 20 °C for 12 h; the mercury was discarded and the green solution was concentrated to ca. 10 mL. Successive addition of 18-crown-6 (37.0 mg, 0.140 mmol) and Na_2dddt (31.0 mg, 0.137 mmol) gave a suspension which was stirred for 30 min at 20 °C. After filtration, dark brown crystals of **4**-thf were formed upon slow diffusion of pentane into the brown solution; the crystals were desolvated into **4** by drying under vacuum. Yield: 104 mg (67%). Anal. Calcd for $\text{C}_{44}\text{H}_{74}\text{NaO}_8\text{S}_4\text{U}$: C, 47.17; H, 6.66; S, 11.45. Found: C, 47.06; H, 6.60; S, 11.35. ^1H NMR (pyridine- d_5 , 23 °C): δ -7.15 (s, 30H, Cp*), 0.14 (s, 4H, dddt), 1.63 (s, 8H, thf), 3.37 (s, 24H, 18-crown-6), 3.67 (s, 8H, thf).

Method 2. An NMR tube was charged with **2** (7.4 mg, 0.011 mmol), 18-crown-6 (2.9 mg, 0.011 mmol), and 2% Na(Hg) (15 mg, 0.013 mmol) in thf- d_8 (0.5 mL). The tube was immersed in an ultrasound bath (80 W, 40 kHz) for 1 h, and the ^1H NMR spectrum of the brown solution showed the almost quantitative formation of **4**. Addition of AgBPh_4 (5.6 mg, 0.013 mmol) gave back **2**.

Synthesis of $[\text{Ce}(\text{Cp}^*)_2\text{Cl}_2\text{K}]$. A flask was charged with CeCl_3 (510 mg, 2.09 mmol), and thf (60 mL) was condensed in. The reaction mixture was refluxed for 12 h, and KCp^* (720 mg, 4.13 mmol) was added to the suspension, which immediately turned yellow and was then stirred for 3 days at 60 °C. The orange solution was filtered and evaporated to dryness, leaving a brown residue which was dried under vacuum. Extraction of the residue with thf (30 mL) gave a light brown-yellow solution. The solvent was evaporated off and replaced with toluene (50 mL). The yellow powder of $[\text{Ce}(\text{Cp}^*)_2\text{Cl}_2\text{K}(\text{thf})]^{12}$ was filtered off and washed with toluene and was transformed into the purple powder of $[\text{Ce}(\text{Cp}^*)_2\text{Cl}_2\text{K}]$ upon drying under vacuum. Yield: 431 mg (40%). Anal. Calcd for $\text{C}_{20}\text{H}_{30}\text{Cl}_2\text{KCe}$: C, 46.14; H, 5.81; Cl, 13.62. Found: C, 46.07; H, 5.70; Cl, 13.86. ^1H NMR (thf- d_8 , 23 °C): δ 4.04 (Cp*). ^1H NMR (pyridine- d_5 , 23 °C): δ 4.41 (Cp*).

Synthesis of $[\text{Nd}(\text{Cp}^*)_2\text{Cl}_2\text{K}]$. A flask was charged with NdCl_3 (450 mg, 1.79 mmol) and KCp^* (620 mg, 3.55 mmol), and thf (50 mL) was condensed in. The reaction mixture was stirred at 20 °C for 10 days. The solvent was evaporated off, and the blue residue was dried under vacuum. The residue was extracted with thf (50 mL), and the blue solution was filtered and evaporated to dryness, leaving the blue powder of $[\text{Nd}(\text{Cp}^*)_2\text{Cl}_2\text{K}]$. Yield: 660 mg (70%). Anal. Calcd for $\text{C}_{20}\text{H}_{30}\text{Cl}_2\text{KNd}$: C, 45.78; H, 5.76; Cl, 13.51. Found: C, 45.52; H, 5.62; Cl, 13.23. ^1H NMR (thf- d_8 , 23 °C): δ 8.55 (Cp*). ^1H NMR (pyridine- d_5 , 23 °C): δ 9.49 (Cp*).

Synthesis of $[\text{Na}(18\text{-crown-6})(\text{thf})_2][\text{Ce}(\text{Cp}^*)_2(\text{dddt})]$. An NMR tube was charged with $[\text{Ce}(\text{Cp}^*)_2\text{Cl}_2\text{K}]$ (9.5 mg, 0.018 mmol) and NaBr (18.4 mg, 0.179 mmol) in thf (0.4 mL). After it was stirred for 2 h at 20 °C, the solution was transferred into another NMR tube and Na_2dddt (4.1 mg, 0.018 mmol) was added; the mixture was stirred at 20 °C for 12 h. The solution was transferred into another NMR tube, and 18-crown-6 (5.1 mg, 0.019 mmol) was added. Pentane was

Table 6. Crystal Data and Structure Refinement Details

	2	4·thf	5	6	7	7·0.5(pentane)	8·0.5(pentane)
empirical formula	C ₂₄ H ₃₄ S ₄ U	C ₄₈ H ₈₂ Na- O ₉ S ₄ U	C ₆₄ H ₁₀₀ Ce ₂ - K ₂ O ₄ S ₈	C ₆₄ H ₁₀₀ K ₂ - Nd ₂ O ₄ S ₈	C ₄₄ H ₇₄ Ce- KO ₁₀ S ₄	C _{46.5} H ₈₀ Ce- KO ₁₀ S ₄	C _{46.5} H ₈₀ K- NdO ₁₀ S ₄
<i>M_r</i>	516.59	1192.40	1548.36	1556.60	1070.49	1106.56	1110.69
cryst syst	orthorhombic	triclinic	monoclinic	monoclinic	monoclinic	triclinic	triclinic
space group	<i>Pnma</i>	<i>P</i> $\bar{1}$	<i>P2</i> ₁ / <i>c</i>	<i>P2</i> ₁ / <i>c</i>	<i>P2</i> ₁ / <i>c</i>	<i>P</i> $\bar{1}$	<i>P</i> $\bar{1}$
<i>a</i> /Å	14.1090(9)	10.4409(8)	13.8911(17)	13.8713(19)	19.6644(14)	16.0585(8)	16.0122(7)
<i>b</i> /Å	42.263(3)	14.6021(11)	16.0128(14)	15.9521(15)	16.4421(11)	16.3685(4)	16.3506(13)
<i>c</i> /Å	12.8230(9)	17.9446(16)	16.037(2)	16.005(2)	16.6911(7)	22.3656(10)	22.3555(17)
α /deg	90	85.219(3)	90	90	90	74.497(3)	74.262(3)
β /deg	90	84.274(5)	98.480(15)	98.245(16)	113.320(4)	74.890(2)	75.035(4)
γ /deg	90	80.661(6)	90	90	90	81.053(3)	80.836(5)
<i>V</i> /Å ³	7646.2(9)	2679.8(4)	3528.1(7)	3505.0(8)	4955.8(5)	5445.8(4)	5417.3(7)
<i>Z</i>	16	2	2	2	4	4	4
<i>T</i> /K	293(2)	100(2)	100(2)	100(2)	100(2)	100(2)	100(2)
<i>D</i> _{calcd} /g cm ⁻³	1.795	1.478	1.458	1.475	1.435	1.350	1.362
μ (Mo K α)/mm ⁻¹	6.705	3.242	1.671	1.865	1.223	1.116	1.240
<i>F</i> (000)	4008	1218	1596	1604	2236	2320	2328
no. of rflns collected	48 642	17 630	26 868	26 373	126 071	137 499	136 374
no. of indep rflns	7505	9266	6702	6546	9327	20 300	20 531
no. of obsd rflns (<i>I</i> > 2 σ (<i>I</i>))	4524	7552	5256	4994	7342	15 998	13 824
<i>R</i> _{int}	0.135	0.053	0.087	0.079	0.063	0.067	0.139
no. of params refined	409	578	371	371	642	1166	1147
<i>R</i> 1	0.053	0.047	0.029	0.027	0.052	0.074	0.062
w <i>R</i> 2	0.135	0.111	0.060	0.062	0.129	0.212	0.191
<i>S</i>	0.899	1.067	0.933	0.866	1.071	1.022	1.062
$\Delta\rho_{\text{min}}$ /e Å ⁻³	-2.09	-1.44	-0.97	-0.71	-1.03	-1.22	-1.06
$\Delta\rho_{\text{max}}$ /e Å ⁻³	1.42	1.84	0.64	0.68	1.08	2.17	1.74

carefully layered onto the solution, and after 3 days, a few orange crystals of [Na(18-crown-6)(thf)₂][Ce(Cp*)₂(dddtt)] were formed.

Synthesis of [Na(18-crown-6)(thf)₂][Nd(Cp*)₂(dddtt)]. An NMR tube was charged with [Nd(Cp*)₂Cl₂K] (6.2 mg, 0.012 mmol) and NaBr (12.9 mg, 0.125 mmol) in thf (0.4 mL). After it was stirred for 2 h at 20 °C, the solution was transferred into another NMR tube and Na₂dddtt (2.8 mg, 0.012 mmol) was added; the mixture was stirred at 20 °C for 5 days. The solution was transferred into another NMR tube, and 18-crown-6 (3.1 mg, 0.012 mmol) was added. Pentane was carefully layered onto the solution, and after 3 days, a few green crystals of [Na(18-crown-6)(thf)₂][Nd(Cp*)₂(dddtt)] were formed.

Synthesis of [{Ce(Cp*)₂(dddtt)K(thf)₂]₂ (5). A flask was charged with [Ce(Cp*)₂Cl₂K] (160 mg, 0.307 mmol) and K₂dddtt (99 mg, 383 mmol), and thf (30 mL) was condensed in; the suspension rapidly turned from yellow to red. After it was stirred for 12 h at 20 °C, the red solution was filtered and the solvent evaporated off. The red powder of **5** was dried under vacuum for only a few minutes because of apparent decomposition upon desolvation. Yield: 180 mg (76%). Anal. Calcd for C₃₂H₅₀KO₂S₄Ce: C, 49.64; H, 6.51; S, 16.57. Found: C, 49.32; H, 6.37; S, 16.75. ¹H NMR (pyridine-*d*₅, 23 °C): δ 0.69 (s, 4H, dddt), 1.63 (s, 8H, thf), 3.67 (s, 8H, thf), 3.97 (s, 30H, Cp*). Crystals were obtained by crystallization from thf.

Synthesis of [{Nd(Cp*)₂(dddtt)K(thf)₂]₂ (6). A flask was charged with [Nd(Cp*)₂Cl₂K] (180 mg, 0.343 mmol) and K₂dddtt (98 mg, 379 mmol), and thf (30 mL) was condensed in; the suspension rapidly turned from blue to green. After it was stirred for 5 days at 20 °C, the green solution was filtered and the solvent evaporated off. The green powder of **6** was dried under vacuum for only a few minutes because of apparent decomposition upon desolvation. Yield: 135 mg (51%). Anal. Calcd for C₃₂H₅₀KO₂S₄Nd: C, 49.38; H, 6.48; S, 16.48. Found: C, 49.13; H, 6.38; S, 16.70. ¹H NMR (pyridine-*d*₅, 23 °C): δ 1.63 (s, 8H, thf), 1.72 (s, 4H, dddt), 3.67 (s, 8H, thf), 7.36 (s, 30H, Cp*). Crystals were obtained by crystallization from thf.

Synthesis of [K(15-crown-5)₂][Ce(Cp*)₂(dddtt)] (7). A flask was charged with **5** (65 mg, 0.084 mmol) and 15-crown-5 (40 mg, 0.177 mmol), and thf (5 mL) was condensed in. The pink solution was frozen, and pentane (10 mL) was layered on it. A few pink-orange crystals of **7** and **7·0.5(pentane)** with

a pink powder of **7** were formed upon slow diffusion of pentane into the thf solution. The powder of **7** was filtered off and dried under vacuum. Yield: 63 mg (70%). Anal. Calcd for C₄₄H₇₄KO₁₀S₄Ce: C, 49.36; H, 6.97; S, 11.98. Found: C, 49.13; H, 6.99; S, 11.69. ¹H NMR (pyridine-*d*₅, 23 °C): δ 0.58 (s, 4H, dddt), 3.56 (s, 40H, 15-crown-5), 3.89 (s, 30H, Cp*).

Synthesis of [K(15-crown-5)₂][Nd(Cp*)₂(dddtt)] (8). A flask was charged with **6** (27 mg, 0.035 mmol) and 15-crown-5 (15 mg, 0.068 mmol), and thf (5 mL) was condensed in. The pink solution was frozen, and pentane (10 mL) was layered on it. A few green crystals of **8·0.5(pentane)** with a green powder of **8** were formed upon slow diffusion of pentane into the thf solution. The powder of **8** was filtered off and dried under vacuum. Yield: 28 mg (75%). ¹H NMR (pyridine-*d*₅, 23 °C): δ 1.83 (s, 4H, dddt), 3.52 (s, 40H, 15-crown-5), 7.22 (s, 30H, Cp*).

Crystallographic Data Collection and Structure Determination. The data for compounds **2**, **5**, and **6** were collected on a Stoe-IPDS imaging plate diffractometer and those for compounds **4·thf**, **7**, **7·0.5(pentane)** and **8·0.5(pentane)** on a Nonius Kappa-CCD area detector diffractometer,³⁴ with graphite-monochromated Mo K α radiation (λ = 0.710 73 Å). The crystals were introduced into glass capillaries with a protecting "Paratone-N" oil (Hampton Research) coating. The unit cell parameters were determined from 10 frames and then refined on all data. The data (φ and ω scans) were processed with DENZO-SMN.³⁵ The structures were solved by direct methods (**2** and **7**) or Patterson map interpretation (all other compounds) with SHELXS-97 and subsequent Fourier-difference synthesis and refined by full-matrix least squares on *F*² with SHELXL-97.³⁶ Absorption effects were corrected empirically with the programs ABSCOR (**2**) and DELABS in PLATON³⁷ (all other compounds).

In compound **2**, one of the two independent molecules is located on a symmetry plane and the two bridging carbon

(34) Kappa-CCD Software; Nonius BV, Delft, The Netherlands, 1998.

(35) Otwinowski, Z.; Minor, W. *Methods Enzymol.* **1997**, *276*, 307.
(36) Sheldrick, G. M. SHELXS-97 and SHELXL-97; University of Göttingen, Göttingen, Germany, 1997.

(37) Spek, A. L. PLATON; University of Utrecht, Utrecht, The Netherlands, 2000.

atoms of the dddd ligand are further disordered over two sites which have been affected with a 0.5 occupancy factor.

In compound **7**, one of the 15-crown-5 moieties, corresponding to atoms O(6)–O(10), was found disordered over two positions rotated by about 20° with respect to one another, which were refined with occupancy parameters constrained to sum to unity (ca. 0.76 and 0.24) and some restraints on bond lengths and displacement parameters.

The structures of the two isomorphous compounds **7**·0.5-(pentane) and **8**·0.5(pentane) could not be refined satisfyingly, which is mainly due to the extended disorder affecting the two 15-crown-5 molecules bound to K(2). The different positions being very badly resolved, only an average position was refined with restraints on bond lengths and displacement parameters. Restraints were also applied for the badly resolved pentane molecule. The atoms C(3) and C(4) pertaining to the dddd ligand labeled A in **7**·0.5(pentane) are disordered over two positions, which were refined with occupancy parameters constrained to sum to unity (ca. 0.66 and 0.34) and some restraints on bond lengths and displacement parameters. In both structures, some voids in the lattice indicate the presence of other, unresolved solvent molecules. In these two compounds, the highest residual electron density peaks are located near the badly resolved crown ether moieties.

The single crystals obtained for the compounds [Na(18-crown-6)(thf)₂][MCP*₂(ddd)] (M = Ce, Nd) were of rather poor quality, and only a rough model of the structure could be obtained. These two compounds are isomorphous and present much disorder in the crown ether and thf molecules. Crystal data for M = Ce: monoclinic, space group *C2/c*, *a* = 52.608(8) Å, *b* = 30.007(3) Å, *c* = 26.782(2) Å, β = 112.092(6)°, *V* = 39174(8) Å³, *Z* = 8, *T* = 100(2) K. Crystal data for M = Nd: monoclinic, space group *C2/c*, *a* = 52.517(3) Å, *b* = 29.807(2) Å, *c* = 26.879(2) Å, β = 112.150(5)°, *V* = 38969(4) Å³, *Z* = 8, *T* = 100(2) K.

All non-hydrogen atoms were refined with anisotropic displacement parameters. Hydrogen atoms were introduced at calculated positions (except for the disordered part in compound **7**) and were treated as riding atoms with a displacement parameter equal to 1.2 (CH₂) or 1.5 (CH₃) times that of the parent atom. Crystal data and structure refinement details are given in Table 6. The molecular plots were drawn with ORTEP-3/POV-Ray.³⁸

Quantum-Chemical Calculations. The computational method we chose to apply is based on relativistic density

functional theory (DFT).³⁹ Indeed, several studies have shown that such DFT calculations permit us to reproduce the experimental geometries of lanthanide and actinide compounds with a satisfying accuracy.³⁰ Our calculations were performed using the Amsterdam Density Functional (ADF2004.01) program.³¹ In this program, scalar relativistic effects are introduced via the zeroth-order regular approximation (ZORA) approach to the Dirac equation.³³ For the open-shell systems, the spin-unrestricted DFT scheme was used. A triple- ζ Slater-type (STO) basis set augmented with one set of polarization functions, i.e., the ADF ZORA/TZP basis set, was employed for all atoms (H, C, S, Ce, and U). A frozen-core approximation was used; the core density is computed relativistically by the Dirac subprogram and is kept frozen during molecular calculations. Core electrons (C.1s) and (S.2p) were frozen for carbon and sulfur, respectively. For the heavy elements cerium and uranium, the valence space contains respectively the 4f/5d/6s/6p (4 valence electrons) and 5f/6s/6p/6d/7s/7p (14 electrons) shells, the frozen cores being (Ce.5p) and (U.5d), but we checked also that the larger uranium (U.6p) core which includes the 6s/6p shells does not lead to a significant electronic structure change of the complexes. Valence electron spin-orbit effects were not taken into account in our work. The Vosko–Wilk–Nusair functional^{40a} for the local density approximation (LDA) and the nonlocal corrections, respectively, for exchange and correlation of Becke^{40b,c} and Perdew^{40d,e} have been used. Molecular orbital plots were generated using the MOLEKEL 4.3 program.⁴¹

Supporting Information Available: Tables of crystal data, atomic positions and displacement parameters, anisotropic displacement parameters, and bond lengths and bond angles in CIF format. This material is available free of charge via the Internet at <http://pubs.acs.org>.

OM050329Z

(39) (a) Baerends, E. J.; Ellis, D. E.; Ros, P. *Chem. Phys.* **1973**, *2*, 41. (b) Versluis, L.; Ziegler, T. *J. Chem. Phys.* **1988**, *88*, 322. (c) te Velde, G.; Baerends, E. J. *J. Comput. Phys.* **1992**, *99*, 84. (d) van Lenthe, E.; Snijders, J. G.; Baerends, E. J. *J. Chem. Phys.* **1996**, *105*, 6505. (e) van Lenthe, E.; Ehlers, A. E.; Baerends, E. J. *J. Chem. Phys.* **1999**, *110*, 8943.

(40) (a) Vosko, S. D.; Wilk, L.; Nusair, M. *Can. J. Chem.* **1990**, *58*, 1200. (b) Becke, A. D. *J. Chem. Phys.* **1986**, *84*, 4524. (c) Becke, A. D. *Phys. Rev. A* **1988**, *38*, 3098. (d) Perdew, J. P. *Phys. Rev. B* **1986**, *33*, 8882. (e) Perdew, J. P. *Phys. Rev. B* **1986**, *33*, 7406.

(41) Flükiger, P.; Lüthi, H. P.; Portmann, S.; Weber, J. MOLEKEL 4.3; Swiss Center for Scientific Computing, Manno, Switzerland, 2000; <http://www.cscs.ch>.

(38) Farrugia, L. J. *J. Appl. Crystallogr.* **1997**, *30*, 565.